ARTICLE

Engineering Persister-Specific Antibiotics with Synergistic Antimicrobial Functions

Nathan W. Schmidt,‡ Stephanie Deshayes,‡ Sinead Hawker, Alyssa Blacker, Andrea M. Kasko,* and Gerard C. L. Wong*

Bioengineering Department, Chemistry and Biochemistry Department, and California NanoSystems Institute, University of California, Los Angeles, 410 Westwood Plaza, Los Angeles, California 90095-1600, United States. ‡N. W. Schmidt and S. Deshayes contributed equally.

ABSTRACT Most antibiotics target growth processes and are ineffective against persister bacterial cells, which tolerate antibiotics due to their reduced metabolic activity. These persisters act as a genetic reservoir for resistant mutants and constitute a root cause of antibiotic resistance, a worldwide problem in human health. We re-engineer antibiotics specifically for persisters using tobramycin, an aminoglycoside antibiotic that targets bacterial ribosomes but is ineffective against persisters with low metabolic and cellular transport activity. By giving tobramycin the ability to induce nanoscopic negative Gaussian membrane curvature *via* addition of 12 amino acids, we transform tobramycin itself into a transporter sequence. The resulting molecule spontaneously permeates membranes, retains the high antibiotic activity of aminoglycosides, kills *E. coli* and *S. aureus* persisters 4−6 logs better than tobramycin, but remains noncytotoxic to eukaryotes. These results suggest a promising paradigm to renovate traditional antibiotics.

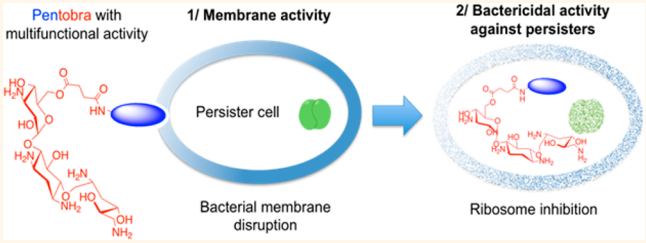

KEYWORDS: antibiotics · cell-penetrating peptide · aminoglycoside · bacterial resistance · drug design

The growing bacterial resistance against our finite repertoire of antibiotics is an urgent global health problem.[1−3] While antibiotic resistance can arise genetically from mutations and horizontal gene transfer,[4] bacteria in an isogenic population are known to display varying susceptibility to antibiotics.[5,6] These bacterial subpopulations provide a phenotypic resistance mechanism whereby a subset of cells with reduced metabolic activity, known as persisters, is tolerant to antibiotic treatment,[5−8] which usually target growth processes like cell-wall, protein, and nucleic acid synthesis. Because persistent bacteria can revert to an actively growing state after antibiotic treatment is ceased,[9,10] this phenotype is a major factor in recurrent and chronic infections.[11,12] Moreover, persistence may assist genetic resistance, as many stress responses that have been implicated in bacterial persistence are also associated with adaptive mutagenesis mechanisms in bacteria,[12] and the continued presence of persisters effectively acts as a reservoir for resistant mutants.[11] Therefore, antibiotics specifically designed against persisters can significantly impact emerging resistance.

We aim to engineer a prototypical persister-specific antibiotic by multiplexing two synergistic antibiotic functions into a single molecule. Tobramycin is a potent aminoglycoside antibiotic shown to target the decoding aminoacyl site on the 16S rRNA component of the 30S ribosomal subunit, leading to mistranslation and cell death.[13,14] However, it has limited activity against persisters, due to attenuation of active bacterial transport mechanisms at low metabolic rates.[15,16] In contrast, antimicrobial peptides (AMPs) kill by selectively disrupting the barrier function of bacterial membranes and/or translocating across membranes like cell-penetrating peptides (CPPs) to bind intracellular targets.[17,18] Importantly, although AMP killing activity is typically lower than that of aminoglycosides, their membrane activity depends less on the metabolic status of the cell.[19] Previous work has shown that tobramycin can retain good activity after conjugation to

* Address correspondence to akasko@ucla.edu; gclwong@seas.ucla.edu.

Received for review April 21, 2014 and accepted July 22, 2014.

Published online August 18, 2014
10.1021/nn502201a

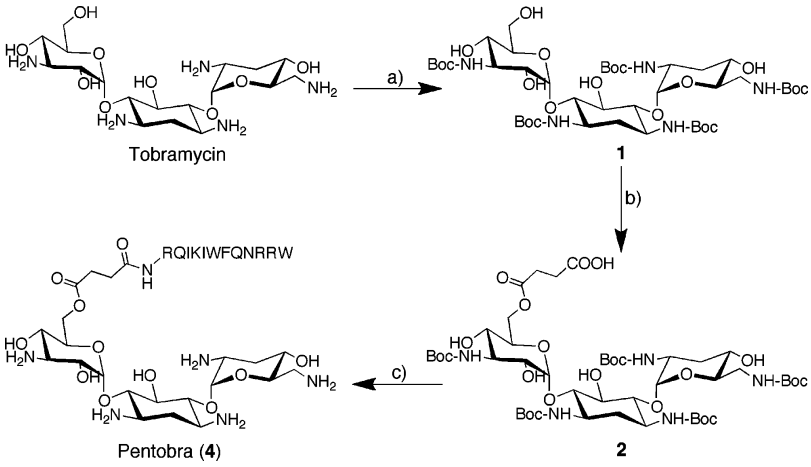

Scheme 1. Synthesis of Pentobra (4): (a) Boc_2O, TEA, H_2O/DMF (1:4), 5 h, 60 °C, 93%; (b) succinic anhydride, DMAP, pyridine, 4 days, 23 °C, 69%; (c) compound 3, DIEA, HBTU, HOBt, DMF, 24 h, 23 °C; (d) TFA/phenol/water/thioanisole/TIS (10:0.7:0.5:0.5:0.25 v/w/v/v/v), 3 h, 23 °C, 49%.

lipid tails,[20,21] and there are a few examples of composite molecules with dual antimicrobial effect.[22] However, there is no general methodology for combining two distinct antimicrobial functions into a single molecule without mutual interference.

We recently showed how the ability to generate the nanoscopic membrane curvature necessary for permeation is "programmed" into AMP sequences, CPP sequences,[23,24] and nonpeptidic membrane-active sequences,[25,26] by examining how patterns in their cationic and hydrophobic compositions relate to the geometric requirements of membrane topology changes. Here, we use this paradigm to program cell-penetrating activity into tobramycin by leveraging its five amine groups and adding a 12-amino acid sequence (see Materials and Methods), so that we effectively have a multifunctional antibiotic that combines membrane-penetrating activity with inhibition of protein synthesis. High-resolution synchrotron X-ray scattering shows that the composite peptide−tobramycin (Pentobra), but not tobramycin, can generate negative Gaussian curvature in model bacteria cell membranes, which is topologically required for membrane permeation mechanisms, such as pore formation, budding, and blebbing.[23,24] The X-ray data are consistent with bacterial inner membrane permeability results from an *E. coli* ML35 reporter strain.[27] Plate killing assays demonstrate the advantage of imparting tobramycin with membrane activity, as Pentobra is able to maintain robust bactericidal activity against *E. coli* and *S. aureus* persister cells, whereas tobramycin was not active. Our results demonstrate that membrane curvature design rules can deterministically inform the construction of multifunctional antibiotics and thereby broaden the spectrum of activity of single target drugs to bacterial subpopulations such as persisters.

RESULTS AND DISCUSSION

Synthesis of Pentobra. The single primary hydroxyl group at the C6″ position in tobramycin was chosen as a point of modification for the peptide−tobramycin conjugate (Scheme 1, compound **4**) due to its expected higher relative reactivity (compared to secondary hydroxyls). Additionally, other groups have previously reported that the primary hydroxyl group of various aminoglycosides including tobramycin is not essential for RNA binding.[13,28−30] First, the five amine groups of tobramycin were protected with *tert*-butyloxycarbonyl (Boc) groups to provide Boc5-tobramycin (compound **1**). Next, the C6″ primary hydroxyl of **1** was selectively reacted with succinic anhydride to introduce a terminal carboxyl function (compound **2**) allowing the coupling with the N-terminal group of the fully protected and resin-anchored peptide (compound **3**). Finally, Pentobra was cleaved off the resin and fully deprotected (cleavage of side-chain protecting groups as well as Boc groups on tobramycin) by treatment with a trifluoroacetic acid mixture containing scavengers.

SAXS Studies. We assayed the membrane restructuring ability of Pentobra using synchrotron small-angle X-ray scattering (SAXS) to determine if Pentobra generates the negative Gaussian membrane curvature necessary for membrane permeabilization.[24] SAXS spectra show that Pentobra significantly restructured small unilamellar vesicles (SUVs) composed of 1,2-dioleoyl-*sn*-glycero-3-phosphoethanolamine (DOPE)/1,2-dioleoyl-*sn*-glycero-3-phospho-L-serine (DOPS) = 80/20 membranes (Figure 1). At a Pentobra to lipid molar ratio, P/L, of 1/80, diffraction peaks at measured Q-positions are observed with characteristic ratios, $\sqrt{2}:\sqrt{3}:\sqrt{4}$, indicating the presence of a *Pn*3*m* cubic phase (a = 18.3 nm). The *Pn*3*m* is a bulk bicontinuous phase composed of two nonintersecting water channels separated by the membrane.[31,32] The bilayer midplane traces out a surface with principle axes of curvature, c_1 and c_2, equal and opposite everywhere; $c_1 = -c_2$. These surfaces are known as minimal surfaces, and they have zero mean curvature, $H = 1/2(c_1 + c_2) = 0$, and negative

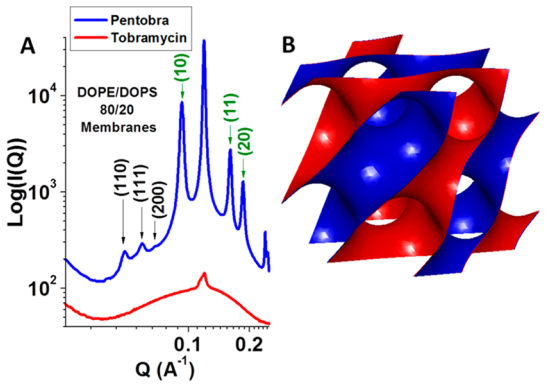

Figure 1. SAXS shows that Pentobra generates negative Gaussian membrane curvature (NGC) necessary for membrane disruption. (A) Spectra from DOPE/DOPS = 80/20 membranes incubated with Pentobra (blue) or tobramycin (red). For Pentobra the presence of a variety of correlation peaks shows that Pentobra can substantially restructure membranes. Peaks with characteristic Q-ratios $\sqrt{2}$:$\sqrt{3}$:$\sqrt{4}$ from (110):(111):(200) reflections indicate that Pentobra induced a *Pn*3*m* cubic phase (lattice parameter a_{Pn3m} = 18.3 nm) that is rich in negative Gaussian curvature. The peaks with characteristic Q-ratios 1:$\sqrt{3}$:2 are the first three (10):(11):(20) reflections from a coexisting inverted hexagonal phase (lattice parameter a_{Hex} = 7.9 nm) that has negative mean curvature. For tobramycin induced NGC is not observed. The antibiotic to lipid molar ratio is 1/80 for Pentobra and 1/40 for tobramycin. (B) Illustration of the *Pn*3*m* cubic phase minimal surface, which has negative Gaussian curvature at every point. The two sides are colored differently to help visualize the surface.

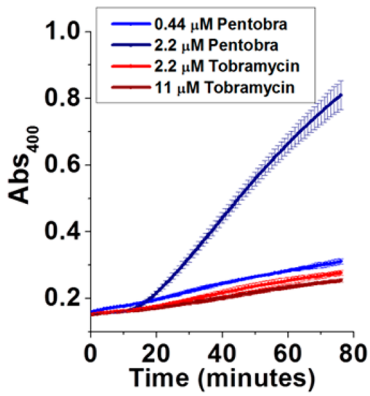

Figure 2. Pentobra permeabilizes *E. coli* cell inner membranes. Measurements of 400 nm light absorbance from ONPG → ONP conversion to assay *E. coli* cell membrane permeabilization by Pentobra and tobramycin. Pentobra permeabilizes *E. coli* membranes in a dose-dependent manner, whereas no membrane permeabilization occurs with tobramycin.

Gaussian curvature (NGC), $K = c_1c_2 < 0$, at every point.[32] Geometrically, everywhere on the surface is locally shaped like a saddle. Observation of Pentobra-induced NGC is significant since NGC is necessary for pore formation, budding, and blebbing.[33] Another set of peaks with Q-positions with characteristic ratios 1:$\sqrt{3}$:2 are also present. They are the first three reflections of an inverted hexagonal phase. This phase consists of hexagonally coordinated water channels wrapped by inverted lipid monolayers. Inverted hexagonal phases have negative mean curvature, which is necessary for NGC. Importantly, tobramycin alone does not induce NGC or negative mean curvature. The spectra for tobramycin and DOPE/DOPS = 80/20 membranes, at molar ratio T/L = 1/40, consist of a broad feature characteristic of a lipid bilayer form factor along with a weak lamellar diffraction peak (d = 5.3 nm) with no new induced membrane curvature. These results are consistent with previous reports that the increase in bacterial membrane permeability following tobramycin treatment is an indirect consequence of tobramycin acting on bacterial ribosomes, leading to membrane incorporation of mistranslated proteins, and not from tobramycin acting directly on the membrane.[34] Importantly, Pentobra has an additional mechanism of selectivity not available to tobramycin: Pentobra has preferential activity against bacterial membranes compared to mammalian membranes, because it selectively permeates membranes enriched in negative spontaneous curvature lipids like those with PE headgroups. This behavior is similar to defensins,[24] CPPs such as the TAT peptide, ANTP penetratin, and polyarginine,[23,35] synthetic cell penetrators,[25] and antimicrobial polymers.[26] For Pentobra the conjoined peptide and tobramycin both influence how this composite molecule interacts with membranes.

***E. coli* ML35 Cell Permeabilization Assays.** To characterize the membrane activity of Pentobra on bacteria, we monitored its permeabilization kinetics on live cells by conducting an enzymatic assay for the conversion of *ortho*-nitrophenyl β-D-galactopyranoside (ONPG) to *ortho*-nitrophenol (ONP) on the *E. coli* strain ML35.[27] *E. coli* ML35 [lacZ-(Con) ΔlacY] constitutively expresses β-galactosidase (β-gal) but lacks the lactose permease necessary for uptake of the lactose analogue ONPG. ONPG internalization cannot occur without a breach in the plasma membrane. Inner membrane permeabilization of *E. coli* ML35 cells allows diffusion of ONPG into cells where β-gal can convert it into ONP, which absorbs at 405 nm.[36] Consistent with its ability to generate NGC, Pentobra induced robust, rapid, dose-dependent permeabilization in *E. coli* ML35 cells (Figure 2). In contrast, permeabilization profiles for tobramycin are comparable to background over a wide range of bactericidal concentrations. The 12 amino acid "Pen" peptide is strongly lytic (Figure S1), as expected from its high hydrophobic content. The addition of cationic tobramycin to the Pen peptide makes the composite molecule less lytic and more selective. Importantly, antibiotic potency did not simply track with membrane permeabilization, as ML35 *E. coli* cells plated following the assay showed colony forming units from the 22 μM Pen peptide condition, whereas no colonies were observed for equivalent molar concentration of Pentobra (Figure S2). Collectively, these results imply that Pentobra can permeabilize bacterial membranes in a manner that depends on the physicochemical properties of both the peptide and tobramycin and that the bactericidal abilities

of Pentobra are not limited to simple membrane permeabilization.

The SAXS data and *E. coli* permeabilization profiles demonstrate that Pentobra, but not tobramycin, can permeate membranes. This gain of function can in principle complement the mechanism of the non-membrane-active template antibiotic. Pentobra can potentially kill *via* interactions with bacterial ribosomes and/or the bacterial membrane. Moreover, Pentobra can actively promote its own uptake into cells without bacterial transport mechanisms. Aminoglycosides must cross membranes in order to reach their bacterial ribosome target,[15,37−39] and their uptake is believed to be energy-dependent from a reliance on the proton-motive force (PMF).[15,40] The poor activity of aminoglycosides against persistent bacteria has been attributed to insufficient PMF,[16] since translation occurs in persister cells at a reduced rate.[7,41] This suggests that multifunctional antibiotics such as Pentobra will have enhanced activity against persisters compared with single-action antibiotics.

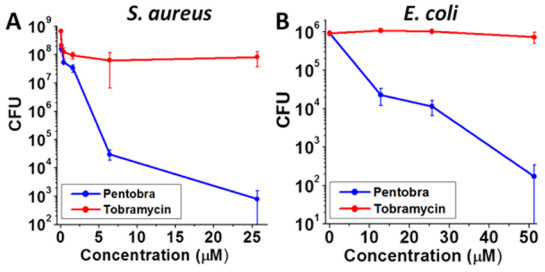

Figure 3. Pentobra displays dose-dependent killing activity against persister cells. (A) *S. aureus* S113 persister cells showed little susceptibility to tobramycin over a wide range of antibiotic concentrations, whereas Pentobra treatment caused a large reduction in cell count (>4 log reduction at >6.4 μM Pentobra). (B) *E. coli* Dh5α persisters are vulnerable to Pentobra and not tobramycin. Pentobra kills persistent *E. coli* at 12.8 μM, and higher Pentobra concentrations lead to further reductions in cell count. Tobramycin is ineffective against *E. coli* persisters at high (>50 μM) antibiotic concentrations.

Bacteria Killing and Cytotoxicity Assays. To test the above idea, we investigated the bactericidal effects of Pentobra against persistent bacteria with plate killing assays. Model Gram positive (*Staphylococcus aureus* S113) and Gram negative (*Escherichia coli* Dh5α) bacteria prepared in a persistent state were incubated for 1.5 h with varying concentrations of Pentobra or tobramycin (Figure 3). Consistent with previous activity profiles of aminoglycosides,[16,42] treatment of *S. aureus* persisters (Figure 3A) with tobramycin led to less than one-log reduction in colony-forming units (CFU), and tobramycin showed poor activity against *E. coli* persisters (Figure 3B) over the entire range of tested concentrations. The advantage of additional membrane activity is apparent, as Pentobra has dose-dependent bactericidal activity against both persistent *S. aureus* and *E. coli* bacteria. *S. aureus* persisters incubated with 1.6 μM Pentobra showed 4-fold reduction in CFU compared with those incubated with an equivalent molar concentration of tobramycin. At higher concentrations the differences between Pentobra and tobramycin become even greater, with 6.4 and 25.7 μM Pentobra producing four-log and six-log reduction in cell counts, respectively. Pentobra was also bactericidal

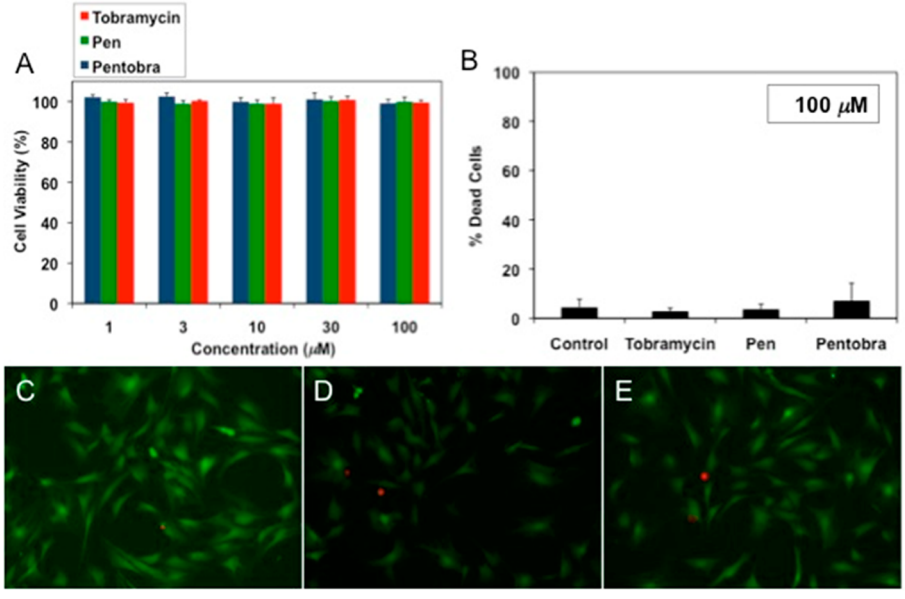

Figure 4. (A) Cell viability of tobramycin, Pen peptide, and Pentobra after 8 h incubation against NIH/3T3 cells using the CellTox Green assay. (B−E) LIVE/DEAD cytotoxicity assay performed on NIH/3T3 cells incubated for 8 h with 100 μM tobramycin, Pen peptide, and Pentobra. (B) Cytotoxicity evaluation (at least 160 cells were counted for each treatment). (C−E) Fluorescence images of stained cells (green fluorescence: live cells, red fluorescence: dead cells) incubated with tobramycin (C), Pen peptide (D), and Pentobra (E).

against *E. coli* persisters, as antibiotic concentrations of 12.8 and 25.7 μM led to 1.5-log and 1.8-log reductions in CFU, respectively, while four-log CFU reductions were observed at 51.3 μM Pentobra, the highest tested concentration. Actively dividing "log phase" bacteria were also highly vulnerable to Pentobra, as single micromolar antibiotic concentrations were bactericidal to *S. aureus* and *E. coli*, and the activity of Pentobra was comparable to tobramycin (potency within a factor of 4; see Figure S3). Importantly, Pentobra concentrations up to 100 μM did not show any cytotoxic effect on NIH/3T3 mouse fibroblast cells after 8 h incubation (Figure 4A), consistent with the fact that its membrane activity is selective. These results suggest that Pentobra is not cytotoxic to mammalian cells at doses and durations where it displays strong antimicrobial activity. In addition, the effect of Pentobra on the cell membrane integrity was evaluated using the LIVE/DEAD cell viability assay. This assay simultaneously determines intracellular esterase activity and plasma membrane integrity using two distinct dyes: (a) calcein, a membrane-permeable polyanionic dye that must be hydrolyzed by intracellular esterases (dead cells lack active esterases) to produce a green fluorescence, and (b) ethidium homodimer, a membrane-impermeable red fluorescent dye that can penetrate only cells with compromised membranes. Treatment of the cells with Pentobra, Pen peptide, and tobramycin resulted in no statistical difference in cytotoxicity (Figure 4B, quantified by counting the percentage of red-stained cells), in agreement with the CellTox green assay. Furthermore, no cells are doubly labeled (both red and green), indicating that the cells maintained their membrane integrity. While Pentobra destabilizes the bacteria membrane, it does not induce any loss of plasma membrane integrity for eukaryotic cells, suggesting that Pentobra is more bacteria specific.

CONCLUSION

In summary, we have engineered a new multifunctional antibiotic that combines membrane activity with inhibition of protein synthesis. This weaponized composite molecule (Pentobra) induced membrane-destabilizing negative Gaussian curvature in model bacterial membranes and permeabilized *E. coli* cell inner membranes. Furthermore, Pentobra showed a strong bactericidal effect against *E. coli* and *S. aureus* persister cells, while free tobramycin failed. The results presented here demonstrate that equipping aminoglycosides with autonomous membrane activity is a viable approach to expand their spectrum of activity to include persisters.

MATERIALS AND METHODS

Synthesis of Boc_5-Tobramycin (1). A solution of tobramycin (5.23 g, 11.2 mmol, 1 equiv) in 108 mL of H_2O/dimethylformamide (DMF) (1:4) was treated with 2 mL of triethylamine (TEA) and di(*tert*-butyl)dicarbonate (Boc_2O) (14.76 g, 67.2 mmol, 6 equiv) and stirred at 60 °C for 5 h. Then, the solution was cooled to room temperature and was concentrated under reduced pressure. The product was precipitated with a few drops of a solution of 30% aqueous ammonia. The precipitate was collected *via* filtration, washed with water, and dried under vacuum overnight (9.93 g, 93%). ^{1}H NMR (300 MHz, MeOH-d_4, 25 °C): δ (ppm) 5.05−5.15 (br, 2H), 3.95 (m, 1H), 3.30−3.90 (br, 15H), 2.13 (m, 1H), 2.01 (m, 1H), 1.65 (q, 1H, J = 12.5 Hz), 1.45 (m, 46H). Mass analysis (MALDI-TOF): m/z 990.526 (calcd for $C_{43}H_{77}NaN_5O_{19}$ $[M + Na]^+$ m/z 990.510).

Synthesis of Compound 2. Compound **1** (3.33 g, 3.44 mmol, 1 equiv), succinic anhydride (379 mg, 3.78 mmol, 1.1 equiv), and dimethylaminopyridine (DMAP) (84 mg, 0.69 mmol, 0.2 equiv) were dissolved in pyridine (14 mL), and the solution was stirred at room temperature for 4 days. The solution was concentrated *via* rotary evaporation, diluted with ethyl acetate (200 mL), washed with brine and saturated $NaHCO_3$ solution (3 × equiv vol), dried with $MgSO_4$, and concentrated to dryness *via* rotary evaporation to yield 2.52 g (69%). ^{1}H NMR (300 MHz, MeOH-d_4, 25 °C): δ (ppm) 5.05−5.15 (br, 2H), 4.30 (m, 1H), 4.19 (m, 1H), 3.95 (m, 1H), 3.30−3.90 (br, 13H), 2.55 (m, 2H), 2.65 (m, 2H), 2.13 (m, 1H), 2.01 (m, 1H), 1.65 (m, 1H), 1.45 (m, 46H). Mass analysis (MALDI-TOF): m/z 1090.511 (calcd for $C_{47}H_{81}NaN_5O_{22}$ $[M + Na]^+$ m/z 1090.527).

Synthesis of Side-Chain-Protected CPP on Resin (3). The (RQIKIWFQNRRW) peptide (Pen) with protected side chains was manually synthesized by solid phase synthesis on 2-chlorotrityl chloride resin (0.84 mmol/g). All following reactions were carried out at room temperature under nitrogen.

Loading of the First Amino Acid. A solution of 9-fluorenylmethoxycarbonyl (Fmoc)−Trp(Boc)−OH (1.11 g, 2.1 mmol, 1.2 equiv) and *N*,*N*-diisopropyl-*N*-ethylamine (DIEA) (1.2 mL, 7.0 mmol, 4 equiv) in dry dichloromethane (DCM) (20 mL) was added to 2-chlorotrityl chloride resin (2.09 g, 1.75 mmol, 1 equiv), and the reaction stirred for 2 h. The resin was transferred into a peptide vessel fitted with a polyethylene filter disk and washed with a solution of DCM/MeOH/DIEA (17:2:1; 3 × 20 mL), DCM (3 × 20 mL), DMF (2 × 20 mL), and DCM (2 × 20 mL). The grafting yield was determined by measuring the absorbance of *N*-(9-fluorenylmethyl)-piperidine complex at 301 nm by UV−vis spectroscopy (after treatment with piperidine) and resulted in 0.35 mmol/g.

Fmoc Removal. The resin (1 equiv) was swollen in DMF (10 mL) for 2 min in a peptide vessel. After draining the solvent, the resin was treated with 20% piperidine in DMF (20 mL) under nitrogen for 30 min and washed with DMF (3 × 20 mL) and DCM (3 × 20 mL). The positive acetaldehyde/chloranil test indicated Fmoc removal.

Coupling. The resin (1 equiv) was swollen in DMF (10 mL) for 2 min, and the solvent was drained. The couplings were done for 4 h with 10 mL of a preactivated (30 min) mixture of Fmoc-protected amino acid (5 equiv), DIEA (10 equiv), 2-(1*H*-benzotriazol-1-yl)-1,1,3,3-tetramethyluronium hexafluorophosphate (HBTU) (5 equiv), and *N*-hydroxybenzotriazole (HOBt) (5 equiv) in DMF. The resin was washed with DMF (3 × 20 mL) and DCM (3 × 20 mL). Couplings were monitored by the acetaldehyde/chloranil test. The final grafting yield was determined by measuring the absorbance of *N*-(9-fluorenylmethyl)piperidine complex at 301 nm by UV−vis spectroscopy (after treatment with piperidine) and resulted in 0.145 mmol/g. The N-terminal Fmoc group was removed as mentioned above to allow further coupling.

Synthesis of Pentobra (4). *Coupling.* The resin **3** (500 mg, 0.073 mmol, 1 equiv) was swollen in DMF (10 mL) for 2 min. After draining the solvent, the resin was treated for 24 h with 10 mL of a preactivated (30 min) mixture of **2** (387 mg, 0.36 mmol, 5 equiv), DIEA (0.12 mL, 0.73 mmol, 10 equiv), HBTU (138 mg, 0.36 mmol, 5 equiv), and HOBt (56 mg, 0.36 mmol, 5 equiv) in DMF. The resin was washed with DMF (3 × 20 mL) and DCM

(3 × 20 mL). The coupling was monitored by the acetaldehyde/chloranil test.

Cleavage of the Peptide from the Resin with Removal of the Acid-Labile Protecting Groups. Peptide cleavage was achieved by using 5 mL of a scavenging mixture of trifluoroacetic acid (TFA)/phenol/water/thioanisole/triisopropylsilane (TIS) (10/0.75/0.5/0.5/0.25 v/w/v/v/v) for 3 h. The resin was filtered out with a fritted filter and rinsed with 1 mL of TFA and 10 mL of DCM. The filtrate containing the unprotected peptide was concentrated to a small volume, and the product was precipitated with cold diethyl ether, isolated by filtration, and dried under vacuum overnight. The peptide was purified by preparative RP-HPLC (reversed-phase high-performance liquid chromatography) (Shimadzu system) at 22 mL/min on a Grace Alltima C_{18} column (250 × 22 mm, 5 mm) using a gradient of A [H_2O + 0.1% TFA] and B [acetonitrile]: 0% B for 5 min, 0% → 70% for 7 min, 70% for 3 min, 70% → 100% for 2 min, and 100% for 2 min; detection at 214 nm; t_r = 12.3 min. Acetonitrile was evaporated under reduced pressure, and the aqueous solution was freeze-dried to give a white solid (78.3 mg, 47%). Mass analysis (MALDI-TOF): *m/z* 2280.329 (calcd for $C_{103}H_{163}N_{32}O_{27}$ $[M + H]^+$ *m/z* 2280.236).

Selection of Pen Peptide. The 12 AA Pen peptide was chosen to ensure that Pentobra (tobramycin + Pen) permeates the cell membranes. Prototypical cell-penetrating peptides and antimicrobial peptides can generate negative Gaussian membrane curvature,[23,24] which is geometrically necessary for membrane destabilizing processes such as pore formation, blebbing, and budding. NGC is a versatile way to compromise the barrier function of cell membranes, and compounds that produce this curvature can permeate cell membranes. The generation of NGC is derived from the lysine, arginine, and hydrophobic content of CPPs and AMPs.[17,23] This implies that compounds with the right proportions of cationic and hydrophobic groups should generate NGC and permeate membranes.

We aimed to design Pentobra with the ability to disrupt membranes and cross them so that it could bind bacterial ribosomes. A CPP-derived design was devised, since these molecules cross membranes and enter cells.[33,43−45] AMPs such as indolicidin, buforin, and tachyplesin can also act as CPPs and kill bacteria by binding to intracellular targets.[46−48] The Pen peptide was derived from the sequence of ANTP penetratin, a well-established cell-penetrating peptide.[49] Penetratin was chosen as a template since it generates saddle-splay curvature,[23] and the sequence of penetratin (RQIKIWFQNRRMKWKK) has a large block of cationic residues; six of the last eight AA are cationic. Tobramycin has five amine groups and carries a cationic charge of +3 to +5 (depending on pH). This implies the amine groups of tobramycin can act as surrogates, so the C-terminal lysines in penetratin were removed. The bulky hydrophobes (2 Ile, 2 Typ, and 1 Phe) were retained since they are important for membrane affinity and curvature generation. In particular, the tryptophans in penetratin have been shown to be important for membrane insertion and cell membrane permeation.[50,51]

SAXS Studies. *Liposome Preparation for X-ray Measurements.* The procedure is the same as described previously.[24] Briefly, DOPE and DOPS lyophilized lipids from Avanti Polar Lipids were used without further purification. SUVs were prepared by sonication. Stock solutions of DOPE and DOPS were prepared in chloroform at ∼20 mg/g. Mixtures of these lipids were prepared at molar ratios, so DOPE/DOPS = 80/20 corresponds to a 4:1 lipid ratio. Chloroform was evaporated under N_2, and the mixtures were dried further by overnight desiccation under vacuum. The dried lipids were resuspended the next day in 100 mM NaCl. Solutions were incubated at 37 °C for 18 h and then sonicated until clear. SUVs were obtained by extrusion (0.2 μm pore Nucleopore filter).

SAXS Experiments. Pentobra and tobramycin stock solutions were prepared by dissolving the molecules in 100 mM NaCl. Lipids were thoroughly mixed with Pentobra/tobramycin at specific molecule to lipid ratios (P/L) in 100 mM NaCl. Sample solutions were hermetically sealed in quartz-glass capillaries (Hilgenberg GmbH, Mark-tubes, code no. 4017515). Synchrotron SAXS experiments were conducted at the Stanford Synchrotron Radiation Laboratory (BL 4-2). Monochromatic X-rays with 9 keV energy were used. Scattering was collected using a Rayonix MX225-HE detector (pixel size 73.2 μm). Samples were also measured at the California NanoSystems Institute (CNSI) at UCLA. A compact light source (Forvis Technologies, Inc.) was used together with a mar345 image plate detector (pixel size 150 μm). Identical samples were prepared and measured at different times and multiple sources to ensure consistency between samples. The 2D SAXS powder patterns were integrated using the Nika 1.48 package[52] for Igor Pro 6.21 and FIT2D.[53]

Bacteria Killing Assays. *Assays on Actively Growing Cells.* *S. aureus* SA113, *E. coli* Dh5α, or *P. aeruginosa* PAO1 cells from freshly streaked Luria-Bertani (LB) broth agar plates were inoculated into tryptic soy broth (TSB) and grown overnight at 37 °C in a shaker incubator into the stationary phase. From the overnight culture, a 100× dilution was incubated at 37 °C for 2−3 h to mid log growth phase (OD_{600} = 0.4−0.6). The mid log phase culture was diluted (roughly 40× for *E. coli*, 25× for *S. aureus*, 68.5× for PA01) to 10^7 CFU/mL in sterile filtered buffer of 10 mM Pipes supplemented with 0.01 volume (1% vol/vol) TSB at pH 7.4 (Pipes/TSB). We inoculated a 20 μL bacteria suspension into 180 μL of buffer containing various concentrations of antibiotic (Pentobra, tobramycin, Pen peptide) in 96-well plates for a total of 2 × 10^5 CFU/well. The plates were sealed with Parafilm, loaded onto microplate shakers, and placed in a 37 °C incubator for 1 h. After incubation, 10-fold serial dilutions were made with Pipes/TSB. Half of each dilution (100 μL) was spotted onto LB agar plates and incubated overnight at 37 °C to yield visible colonies. *S. aureus* and *E. coli* killing assays were done in quadruplicate for Pentobra and triplicate for tobramycin. The results from one assay performed in duplicate are shown and are characteristic of the trends observed in all assays. For *S. aureus* a total of three assays were done with Pen peptide, and the results are shown for one assay performed in duplicate. Data for *P. aeruginosa* are representative of killing from three separate experiments.

Persister Cell Assays. The procedure for preparing *S. aureus* SA113 and *E. coli* Dh5α persister cells is based on previous protocols.[10,16] Cells from freshly streaked agar plates were inoculated in 1 mL of TSB and incubated for 16 h at 37 °C in a shaker incubator to obtain stationary phase cultures. Nonpersister cells were eliminated by adding ampicillin to a final concentration of 100 μg/mL, followed by a 3 h incubation at 37 °C. Previous work has shown that this treatment causes lysis of a subset of the cell population.[10]

E. coli cells were pelleted (5000 rpm for 5 min), washed in M9 minimal media, and resuspended in M9 minimal media to a final bacteria stock solution of 5 × 10^7 CFU/mL. We inoculated a 20 μL *E. coli* suspension into 180 μL of M9 media containing various concentrations of antibiotic (Pentobra, tobramycin) in 96-well plates for a total of 10^6 CFU/well. The plates were sealed with Parafilm, loaded onto microplate shakers, and placed in a 37 °C incubator for 1.5 h. After incubation, 10-fold serial dilutions were made with M9 media. Half of each dilution (100 μL) was spotted onto LB agar plates and incubated overnight at 37 °C to yield visible colonies. The *E. coli* persister assays were performed in quadruplicate.

S. aureus cells were diluted 10× into 10 mM Pipes at pH 7.4 buffer for a bacteria stock solution of roughly 10^9 CFU/mL. We inoculated a 20 μL *S. aureus* suspension into 180 μL of Pipes buffer containing various concentrations of antibiotic (Pentobra, tobramycin) in 96-well plates for a total of ∼10^8 CFU/well. The plates were sealed with Parafilm, loaded onto microplate shakers, and placed in a 37 °C incubator for 1.5 h. After incubation, 10-fold serial dilutions were made in Pipes buffer. Half of each dilution (100 μL) was spotted onto LB agar plates and incubated overnight at 37 °C to yield visible colonies. The *S. aureus* persister assays were performed in triplicate. The data shown are averages from two independent trials and are representative of the three assays.

***E. coli* ML35 Cell Permeabilization Assays.** *E. coli* ML35 [lacZ-(Con) ΔlacY] cannot take up lactose mimic ONPG unless cell membrane integrity is compromised. Upon membrane permeabilization, ONPG can diffuse into the bacterial cell cytoplasm, where it is hydrolyzed by β-galactosidase into galactose and

ONP. Since ONP absorbs at 400 nm, the permeabilization kinetics of membrane-disrupting agents can be monitored by OD_{400} absorbance measurement. The methodology here is very similar to previous studies.[36] Log-phase *E. coli* cells were grown as described above and washed and resuspended in 10 mM Tris supplemented with 0.01 volume (1% vol/vol) TSB at pH 7.4 (Tris-TSB). In triplicate, bacteria (5×10^6 cells/well) were exposed to various concentrations of antibiotic (Pentobra, tobramycin, Pen peptide) in the presence of 2.5 mM ONPG for 90 min at 37 °C. The kinetics of ONPG hydrolysis were measured by determining the absorbance at 400 nm using a plate reader spectrophotometer.

Cytotoxicity Assays. *CellTox Green Assay.* The cytotoxicity of Pentobra was investigated on NIH/3T3 cells (ATCC) using the CellTox Green assay (Promega, USA). Cells were seeded in a 96-well plate at a concentration of 2.5×10^3 cells/well. Then 100 μL of DMEM media was added to each well containing 0.2% CellTox Green dye and varying concentrations of Pentobra, CPP, or tobramycin and incubated for 8 and 24 h before the plate was read using an excitation wavelength of 485 nm and emission filter of 535 nm on a microplate reader (Beckman Coulter, DTX 880 multimode detector). A lysis solution, known to be toxic to the cells, has been used as a positive control and represents the maximum dead cell signal obtainable from nonproliferating cells. The untreated cell population represents the maximal negative control signal obtainable at the end of an exposure period. The fluorescence values were normalized (from positive and negative controls) and converted to corresponding viability values.

LIVE/DEAD Viability Assay. The effect of Pentobra on the plasma membrane integrity was investigated on NIH/3T3 cells using the LIVE/DEAD viability/cytotoxicity kit (Molecular Probes). Briefly, 50 000 cells/well were incubated in a 24-well plate and treated with 100 μM tobramycin, Pen peptide, or Pentobra for 8 h at 37 °C. Then, the cells were stained with 100 μL of the LIVE/DEAD assay reagents (2 μM calcein and 4 μM ethidium homodimer) and incubated at 37 °C for 20 min. The labeled cells were counted using a Zeiss Axiovert Observer Z1 inverted fluorescent microscope (at least 160 cells were counted for each treatment).

Conflict of Interest: The authors declare no competing financial interest.

Supporting Information Available: Supplementary figures for membrane permeabilization and microbicidal assays are provided. This material is available free of charge *via* the Internet at http://pubs.acs.org.

Acknowledgment. We thank A. Ouellette for the ML35 strain, D. Wong for assistance with the 3T3 viability studies, and N. Garg and B. Wu for use of their facilities. We also thank Melissa Johnson and Jay Abraham for help with *E. coli* killing assays. SAXS was performed at the Stanford Synchrotron Radiation Lightsource, supported by the U.S. Department of Energy, Basic Energy Sciences, under Contract No. DE-AC02-76SF00515, and at the UCLA CNSI. This work is supported by NIH grant 1UO1 AI082192-01 (G.C.L.W.), NSF grant DMR1106106 (G.C.L.W.), and NIH grant 1-DP2-OD008533 (A.M.K.).

REFERENCES AND NOTES

1. CDC Threat Report **2013**.
2. Dantes, R.; Mu, Y.; Belflower, R.; Aragon, D.; Dumyati, G.; Harrison, L. H.; Lessa, F. C.; Lynfield, R.; Nadle, J.; Petit, S.; *et al.* National Burden of Invasive Methicillin-Resistant Staphylococcus Aureus Infections, United States, 2011. *JAMA Int. Med.* **2013**, *173*, 1970–1978.
3. Taubes, G. The Bacteria Fight Back. *Science* **2008**, *321*, 356–361.
4. Ochman, H.; Lawrence, J. G.; Groisman, E. A. Lateral Gene Transfer and the Nature of Bacterial Innovation. *Nature* **2000**, *405*, 299–304.
5. Balaban, N. Q.; Merrin, J.; Chait, R.; Kowalik, L.; Leibler, S. Bacterial Persistence as a Phenotypic Switch. *Science* **2004**, *305*, 1622–1625.
6. Lewis, K. Persister Cells, Dormancy and Infectious Disease. *Nat. Rev. Microbiol.* **2007**, *5*, 48–56.
7. Gefen, O.; Gabay, C.; Mumcuoglu, M.; Engel, G.; Balaban, N. Q. Single-Cell Protein Induction Dynamics Reveals a Period of Vulnerability to Antibiotics in Persister Bacteria. *Proc. Natl. Acad. Sci. U.S.A.* **2008**, *105*, 6145–6149.
8. Gefen, O.; Balaban, N. Q. The Importance of Being Persistent: Heterogeneity of Bacterial Populations under Antibiotic Stress. *FEMS Microbiol. Rev.* **2009**, *33*, 704–717.
9. Bigger, J. Treatment of Staphylococcal Infections with Penicillin by Intermittent Sterilisation. *Lancet* **1944**, *244*, 497–500.
10. Keren, I.; Kaldalu, N.; Spoering, A.; Wang, Y.; Lewis, K. Persister Cells and Tolerance to Antimicrobials. *FEMS Microbiol. Lett.* **2004**, *230*, 13–18.
11. Mulcahy, L. R.; Burns, J. L.; Lory, S.; Lewis, K. Emergence of Pseudomonas Aeruginosa Strains Producing High Levels of Persister Cells in Patients with Cystic Fibrosis. *J. Bacteriol.* **2010**, *192*, 6191–6199.
12. Lewis, K. Persister Cells. *Annu. Rev. Microbiol.* **2010**, *64*, 357–372.
13. Vicens, Q.; Westhof, E. Crystal Structure of a Complex between the Aminoglycoside Tobramycin and an Oligonucleotide Containing the Ribosomal Decoding A Site. *Chem. Biol.* **2002**, *9*, 747–755.
14. Fourmy, D.; Recht, M. I.; Blanchard, S. C.; Puglisi, J. D. Structure of the a Site of Escherichia Coli 16s Ribosomal RNA Complexed with an Aminoglycoside Antibiotic. *Science* **1996**, *274*, 1367.
15. Davis, B. D. Mechanism of Bactericidal Action of Aminoglycosides. *Microbiol. Rev.* **1987**, *51*, 341.
16. Allison, K. R.; Brynildsen, M. P.; Collins, J. J. Metabolite-Enabled Eradication of Bacterial Persisters by Aminoglycosides. *Nature* **2011**, *473*, 216–220.
17. Schmidt, N. W.; Wong, G. C. Antimicrobial Peptides and Induced Membrane Curvature: Geometry, Coordination Chemistry, and Molecular Engineering. *Curr. Opin. Solid State Mater. Sci.* **2013**, *17*, 151–163.
18. Brogden, K. A. Antimicrobial Peptides: Pore Formers or Metabolic Inhibitors in Bacteria? *Nat. Rev. Microbiol.* **2005**, *3*, 238–250.
19. Hurdle, J. G.; O'Neill, A. J.; Chopra, I.; Lee, R. E. Targeting Bacterial Membrane Function: An Underexploited Mechanism for Treating Persistent Infections. *Nat. Rev. Microbiol.* **2011**, *9*, 62–75.
20. Bera, S.; Zhanel, G. G.; Schweizer, F. Design, Synthesis, and Antibacterial Activities of Neomycin-Lipid Conjugates: Polycationic Lipids with Potent Gram-Positive Activity. *J. Med. Chem.* **2008**, *51*, 6160–6164.
21. Dhondikubeer, R.; Bera, S.; Zhanel, G. G.; Schweizer, F. Antibacterial Activity of Amphiphilic Tobramycin. *J. Antibiot.* **2012**, *65*, 495–498.
22. Bryskier, A. Dual B-Lactam-Fluoroquinolone Compounds: A Novel Approach to Antibacterial Treatment. *Expert Opin. Invest. Drugs* **1997**, *6*, 1479–1499.
23. Mishra, A.; Lai, G. H.; Schmidt, N. W.; Sun, V. Z.; Rodriguez, A. R.; Tong, R.; Tang, L.; Cheng, J.; Deming, T. J.; Kamei, D. T.; *et al.* Translocation of HIV Tat Peptide and Analogues Induced by Multiplexed Membrane and Cytoskeletal Interactions. *Proc. Natl. Acad. Sci. U.S.A.* **2011**, *108*, 16883–16888.
24. Schmidt, N. W.; Mishra, A.; Lai, G. H.; Davis, M.; Sanders, L. K.; Tran, D.; Garcia, A.; Tai, K. P.; McCray, P. B., Jr.; Ouellette, A. J. Criterion for Amino Acid Composition of Defensins and Antimicrobial Peptides Based on Geometry of Membrane Destabilization. *J. Am. Chem. Soc.* **2011**, *133*, 6720–6727.
25. Schmidt, N. W.; Lis, M.; Zhao, K.; Lai, G. H.; Alexandrova, A. N.; Tew, G. N.; Wong, G. C. Molecular Basis for Nanoscopic Membrane Curvature Generation from Quantum Mechanical Models and Synthetic Transporter Sequences. *J. Am. Chem. Soc.* **2012**, *134*, 19207–19216.
26. Hu, K.; Schmidt, N. W.; Zhu, R.; Jiang, Y.; Lai, G. H.; Wei, G.; Palermo, E. F.; Kuroda, K.; Wong, G. C.; Yang, L. A Critical Evaluation of Random Copolymer Mimesis of Homogeneous Antimicrobial Peptides. *Macromolecules* **2013**, *46*, 1908–1915.
27. Lehrer, R. I.; Barton, A.; Ganz, T. Concurrent Assessment of Inner and Outer Membrane Permeabilization and

Bacteriolysis in E. coli by Multiple-Wavelength Spectrophotometry. *J. Immunol. Methods* **1988**, *108*, 153–158.
28. Asensio, J. L.; Hidalgo, A.; Bastida, A.; Torrado, M.; Corzana, F.; Chiara, J. L.; Garcia-Junceda, E.; Canada, J.; Jimenez-Barbero, J. A Simple Structural-Based Approach to Prevent Aminoglycoside Inactivation by Bacterial Defense Proteins. Conformational Restriction Provides Effective Protection against Neomycin-B Nucleotidylation by Ant4. *J. Am. Chem. Soc.* **2005**, *127*, 8278–8279.
29. Hanessian, S.; Masse, R.; Capmeau, M. L. Aminoglycoside Antibiotics: Synthesis of 5″-Amino 5″-Deoxyneomycin and 5″-Amino-5″-Deoxyparamomycin. *J. Antibiot.* **1977**, *30*, 893–896.
30. Michael, K.; Tor, Y. Modifying Aminoglycoside Antibiotics. In *RNA-Binding Antibiotics*; Wallis, R. S. a. M. G., Ed.; Landes Bioscience, 2000.
31. Schwarz, U. S.; Gompper, G. Stability of Inverse Bicontinuous Cubic Phases in Lipid-Water Mixtures. *Phys. Rev. Lett.* **2000**, *85*, 1472–1475.
32. Shearman, G.; Ces, O.; Templer, R.; Seddon, J. Inverse Lyotropic Phases of Lipids and Membrane Curvature. *J. Phys.: Condens. Matter* **2006**, *18*, S1105.
33. Schmidt, N.; Mishra, A.; Lai, G. H.; Wong, G. C. Arginine-Rich Cell-Penetrating Peptides. *FEBS Lett.* **2010**, *584*, 1806–1813.
34. Davis, B. D.; Chen, L. L.; Tai, P. C. Misread Protein Creates Membrane Channels: An Essential Step in the Bactericidal Action of Aminoglycosides. *Proc. Natl. Acad. Sci. U.S.A.* **1986**, *83*, 6164–6168.
35. Mishra, A.; Gordon, V. D.; Yang, L.; Coridan, R.; Wong, G. C. Hiv Tat Forms Pores in Membranes by Inducing Saddle-Splay Curvature: Potential Role of Bidentate Hydrogen Bonding. *Angew. Chem., Int. Ed.* **2008**, *47*, 2986–2989.
36. Llenado, R. A.; Weeks, C. S.; Cocco, M. J.; Ouellette, A. J. Electropositive Charge in A-Defensin Bactericidal Activity: Functional Effects of Lys-for-Arg Substitutions Vary with the Peptide Primary Structure. *Infect. Immun.* **2009**, *77*, 5035–5043.
37. Magnet, S.; Blanchard, J. S. Molecular Insights into Aminoglycoside Action and Resistance. *Chem. Rev. (Washington, DC, U. S.)* **2005**, *105*, 477–498.
38. Kohanski, M. A.; Dwyer, D. J.; Wierzbowski, J.; Cottarel, G.; Collins, J. J. Mistranslation of Membrane Proteins and Two-Component System Activation Trigger Antibiotic-Mediated Cell Death. *Cell* **2008**, *135*, 679–690.
39. Vakulenko, S. B.; Mobashery, S. Versatility of Aminoglycosides and Prospects for Their Future. *Clin. Microbiol. Rev.* **2003**, *16*, 430–450.
40. Taber, H. W.; Mueller, J.; Miller, P.; Arrow, A. Bacterial Uptake of Aminoglycoside Antibiotics. *Microbiol. Rev.* **1987**, *51*, 439.
41. Shah, D.; Zhang, Z.; Khodursky, A. B.; Kaldalu, N.; Kurg, K.; Lewis, K. Persisters: A Distinct Physiological State of E. coli. *BMC Microbiol.* **2006**, *6*, 53.
42. Spoering, A. L.; Lewis, K. Biofilms and Planktonic Cells of Pseudomonas Aeruginosa Have Similar Resistance to Killing by Antimicrobials. *J. Bacteriol.* **2001**, *183*, 6746–6751.
43. Snyder, E.; Dowdy, S. Cell Penetrating Peptides in Drug Delivery. *Pharm. Res.* **2004**, *21*, 389–393.
44. Zorko, M.; Langel, U. Cell-Penetrating Peptides: Mechanism and Kinetics of Cargo Delivery. *Adv. Drug Delivery Rev.* **2005**, *57*, 529–545.
45. Lindgren, M.; Hällbrink, M.; Prochiantz, A.; Langel, U. Cell-Penetrating Peptides. *Trends Pharmacol. Sci.* **2000**, *21*, 99–103.
46. Hsu, C.-H.; Chen, C.; Jou, M.-L.; Lee, A. Y.-L.; Lin, Y.-C.; Yu, Y.-P.; Huang, W.-T.; Wu, S.-H. Structural and DNA-Binding Studies on the Bovine Antimicrobial Peptide, Indolicidin: Evidence for Multiple Conformations Involved in Binding to Membranes and DNA. *Nucleic Acids Res.* **2005**, *33*, 4053–4064.
47. Park, C. B.; Kim, H. S.; Kim, S. C. Mechanism of Action of the Antimicrobial Peptide Buforin II: Buforin Ii Kills Microorganisms by Penetrating the Cell Membrane and Inhibiting Cellular Functions. *Biochem. Biophys. Res. Commun.* **1998**, *244*, 253–257.
48. Yonezawa, A.; Kuwahara, J.; Fujii, N.; Sugiura, Y. Binding of Tachyplesin I to DNA Revealed by Footprinting Analysis: Significant Contribution of Secondary Structure to DNA Binding and Implication for Biological Action. *Biochemistry* **1992**, *31*, 2998–3004.
49. Derossi, D.; Chassaing, G.; Prochiantz, A. Trojan Peptides: The Penetratin System for Intracellular Delivery. *Trends Cell Biol.* **1998**, *8*, 84–87.
50. Derossi, D.; Joliot, A. H.; Chassaing, G.; Prochiantz, A. The Third Helix of the Antennapedia Homeodomain Translocates through Biological Membranes. *J. Biol. Chem.* **1994**, *269*, 10444–10450.
51. Dom, G.; Shaw-Jackson, C.; Matis, C.; Bouffioux, O.; Picard, J. J.; Prochiantz, A.; Mingeot-Leclercq, M. P.; Brasseur, R.; Rezsohazy, R. Cellular Uptake of Antennapedia Penetratin Peptides Is a Two-Step Process in Which Phase Transfer Precedes a Tryptophan-Dependent Translocation. *Nucleic Acids Res.* **2003**, *31*, 556–561.
52. usaxs.xor.aps.anl.gov/staff/ilavsky/nika.html.
53. www.esrf.eu/computing/scientific/FIT2D/.